SPE 56522

Comprehensive Mechanistic Modeling of Two-Phase Flow in Deviated Wells

A. S. Kaya, SPE, The University of Tulsa; C. Sarica, SPE, The Pennsylvania State University; and J. P. Brill, SPE, The University of Tulsa

Abstract

A new comprehensive mechanistic model was developed to predict flow pattern and flow characteristics such as pressure drop and liquid holdup in vertical and deviated wells. The model includes five flow patterns: bubbly, dispersed bubble, slug, churn and annular flows.

Flow pattern prediction incorporates the transition models proposed by Barnea[1] (or Taitel et al.[2]) for dispersed bubble flow, Ansari et al.[3] for annular flow, Tengesdal et al.[4] for churn flow, and a new bubbly flow transition model. For each predicted flow pattern, a separate hydrodynamic mechanistic model is proposed. A new hydrodynamic model for bubbly flow has been developed, and the Chokshi[5] slug flow model has been modified significantly. The Tengesdal et al. and Ansari et al. models have been adopted for churn and annular flows, respectively.

The comprehensive model is evaluated using a well databank of 2,052 cases covering a broad range of field data. Pressure drop predictions with the model are also compared with those using the Ansari et al., Chokshi, Hasan and Kabir[6], and Tengesdal mechanistic models, and the Aziz et al.[8], and Hagedorn and Brown[9] correlations. The results of the comparison study show that the proposed comprehensive mechanistic model performs the best and agrees with the data.

Introduction

Two-phase flow occurs commonly in the petroleum, chemical, civil and nuclear industries. In the petroleum industry, two-phase flow is encountered in oil and gas production, transportation and processing systems. The complex nature of two-phase flow challenges production engineers with problems of understanding, analyzing and modeling two-phase flow systems.

Because of the complex nature of two-phase flow in pipes, the prediction of pressure drop in producing wells was first approached through empirical correlations. The trend has shifted in recent years to the modeling approach. The fundamental postulate of the modeling approach is the existence of flow patterns that can be identified by a typical geometrical arrangement of the phases in the pipe. Each flow pattern exhibits a characteristic spatial distribution of the interface(s), flow mechanisms and distinctive values for such design parameters as pressure gradient, holdup and heat transfer coefficients. Various mechanistic models have been developed to predict flow patterns. For each flow pattern, separate models were developed to predict such flow characteristics as holdup and pressure drop. By considering basic fluid mechanics, the resulting models can be applied with more confidence to flow conditions other than those used for their development.

Early modeling efforts concentrated on vertical wells. Although one can use vertical flow models for deviated wells by simply applying an inclination angle correction to the gravity component of the pressure gradient equation, the results should be used with caution, and are not expected to reflect the actual flow behavior. Therefore, it was recognized that additional studies were needed to improve predictions for deviated wells.

The main purpose of this study was to develop a new comprehensive mechanistic model, first to predict flow pattern, and then to calculate the characteristics of two-phase flow in vertical and deviated wells by applying separate hydrodynamic models for each flow pattern. The proposed model was evaluated against the expanded TUFPP well data bank and compared with other commonly used and better performing mechanistic models and correlations.

Flow Pattern Prediction Models

Taitel et al.[2] theoretically and experimentally studied and identified five distinct flow patterns for vertical upward flow: bubbly, dispersed bubble, slug, churn and annular flow (Fig. 1). Later, Shoham[10] also verified these flow patterns for inclined pipes. A unified flow pattern prediction method was developed by Barnea[1] to cover the entire range of inclination

angles. The following section contains the descriptions of transition mechanisms between flow patterns and mathematical models proposed for these transitions.

Bubbly to Slug Flow Transition. Bubble flow is characterized by a gas phase distributed as small bubbles in a continuous liquid phase. Based on the presence or absence of relative velocity or slippage between the two phases, bubble flow can further be classified into bubbly and dispersed bubble flows (Fig. 2). In upward flow, bubbly flow is observed only in relatively large diameter, vertical and inclined pipes. In bubbly flow, bubbles tend to flow near the upper part of inclined pipes because of slippage and buoyancy effects (Fig. 2-A).

For bubbly flow, Taitel et al.[2] presented a minimum pipe diameter expression as the existence criterion. This criterion is based on the comparison between rise velocity of elongated bubbles and small bubbles, and is given by the following expression:

$$D_{mn} = 19.01\left[\frac{\sigma(\rho_L - \rho_G)}{\rho_L^2 g}\right] \quad\text{.........................} (1)$$

Barnea et al.[11] postulated that the inclination angle from the horizontal should be large enough to prevent migration of bubbles to the top wall of the pipe. The critical inclination angle can then be obtained by using the balance between buoyancy and drag forces acting on a single bubble. The resulting expression is given as:

$$\frac{\cos\theta}{\sin^2\theta} = \frac{3}{4}\cos 45°\frac{v_{bs}^2}{g}\left(\frac{0.968}{D}\right) \quad\text{.......................} (2)$$

Where v_{bs} is the rise velocity of bubbles in a stagnant liquid column given by the following expression[12].

$$v_{bs} = 1.53\left[\frac{g\sigma(\rho_L - \rho_G)}{\rho_L^2}\right]^{0.25} \quad\text{..........................} (3)$$

A volumetric packing density of $\alpha = 0.25$ is taken as the criterion for transition from bubbly to slug flow[2]. A new bubble slip velocity expression has been developed for modeling of this transition boundary equation (line A in Fig. 1). The development of the expression is given in the Appendix-A. The definition of slip velocity at the transition condition is used to find the transition equation, which is expressed in terms of superficial velocities as:

$$v_{SG} = 0.333v_{SL} + 0.3825\left[\frac{g\sigma(\rho_L - \rho_G)}{\rho_L^2}\right]^{0.25}\sqrt{\sin\theta} \quad\text{.........} (4)$$

Dispersed Bubble Flow Transition. The first transition mechanism from dispersed bubble flow was proposed by Taitel et al.[2] for upward vertical flow. They suggested that dispersed bubble flow occur when turbulent forces are strong

enough to overcome the interfacial tension to disperse the gas phase into small spherical bubbles. They used Hinze's[13] theory for break up of immiscible fluid phases by turbulent forces at low concentrations of the dispersed phase. The maximum stable diameter of a dispersed bubble is expressed as

$$d_{mx} = \left[4.15\left(\frac{v_{SG}}{v_M}\right)^{0.5} + 0.725\right]\left(\frac{\sigma}{\rho_L}\right)^{0.6}\left(\frac{2f_M}{D}\rho_M v_M^2\right)^{-0.4} (5)$$

If the maximum stable bubble size is smaller than the critical diameter, dispersed bubble flow exists (line B in Fig. 1). The critical bubble diameter, above which a gas bubble is deformed, has been expressed as

$$d_{CD} = 2\left(\frac{0.4\sigma}{(\rho_L - \rho_G)g}\right)^{0.5} \quad\text{...........................} (6)$$

Barnea[14] modified the Taitel et al.[2] model to account for inclination angle. She also extended it into a unified model by comparing maximum stable bubble size with a critical diameter, below which migration of bubbles to the upper part of the pipe is prevented. The critical diameter is given as

$$d_{CB} = \frac{3}{8}\frac{\rho_L}{\rho_L - \rho_G}\frac{f_M v_M^2}{g\cos\theta} \quad\text{..............................} (7)$$

However, at high gas flow rates, the transition boundary described above is terminated by another mechanism called the maximum volumetric packing (line C in Fig. 1). This mechanism states that turbulent forces cannot prevent agglomeration once the void fraction reaches 0.52. The no-slip holdup definition is used to identify this transition boundary, which is evaluated with a critical value of 0.48, and the following transition boundary equation is then obtained[2].

$$v_{SG} = 1.083v_{SL} \quad\text{.....................................} (8)$$

Slug to Churn Transition. Tengesdal et al.[4] have recently completed a thorough analysis of churn flow. They proposed a new transition criterion based on a drift flux approach for vertical and inclined pipes. The global void fraction in a slug unit can be expressed by the following equation:

$$\alpha = v_{SG}/(1.2v_M + v_o) \quad\text{................................} (9)$$

Where v_o, the Taylor bubble rise velocity, is given by Bendiksen[15] as

$$v_o = \left[0.35\sin\theta + 0.54\cos\theta\left(\frac{g(\rho_L - \rho_G)D}{\rho_L}\right)^{0.5}\right] \quad\text{......} (10)$$

Owen[16] found experimentally that this transition occurs at a void fraction of about 0.78 in the Taylor bubble region. Tengesdal et al. proposed that the void fraction in the Taylor bubble region could be taken as the global void fraction at the transition. Substituting $\alpha = 0.78$ into Eq. 9 and solving for V_{SG} yields the slug to churn transition criterion (line D in Fig. 1).

$$v_{SG} = 12.19 \left(1.2 v_{SL} + v_o \right) \dots\dots\dots (11)$$

Transition from Annular Flow. Recently, Kaya *et al.*[17] have completed a thorough review of available annular flow transition models. They showed that, for high pressure and high temperature conditions, the modified Ansari *et al.*[3] transition model performs the best and was adopted in the present study.

Barnea[14] attributed the annular flow transition to blockage of the gas core. She postulated that the blockage might result from two possible mechanisms; instability of the liquid film and bridging of the gas core.

At low liquid flow rates, the liquid film becomes unstable because of the low core shear stress, resulting in downward flow of the film and blockage of the gas core.

Instability of the film (line E in Fig. 1) occurs when

$$Y_M \geq \frac{2 - 1.5 H_{LF}}{H_{LF}^3 \left(1 - 1.5 H_{LF} \right)} X_M^2 \quad \dots\dots\dots (12)$$

H_{LF} is the fraction of the pipe cross section that is occupied by the liquid film and can be expressed in terms of the minimum dimensionless film thickness, $\underline{\delta}$, as

$$H_{LF} = 4\underline{\delta}\left(1 - \underline{\delta}\right) \dots\dots\dots (13)$$

$\underline{\delta}$ can be obtained from the following combined momentum equation:

$$Y_M - \frac{Z}{4\underline{\delta}\left(1 - \underline{\delta}\right)\left[1 - 4\underline{\delta}\left(1 - \underline{\delta}\right)\right]^{2.5}} + \frac{X_M^2}{\left[4\underline{\delta}\left(1 - \underline{\delta}\right)\right]^3} = 0 \quad \dots\dots (14)$$

Y_M and X_M are the modified Lockhart-Martinelli[18] parameters, expressed as

$$X_M = \sqrt{\left(1 - FE\right)^2 \frac{f_F}{f_{SL}} \frac{(dp/dL)_{SL}}{(dp/dL)_{SC}}} \quad \dots\dots\dots (15)$$

$$Y_M = \frac{g \sin\theta \left(\rho_L - \rho_C\right)}{(dp/dL)_{SC}} \quad \dots\dots\dots (16)$$

The superficial frictional pressure gradients for liquid and the gas core are respectively given as;

$$(dp/dL)_{SL} = f_{SL} \rho_L v_{SL}^2 / (2D) \dots\dots\dots (17)$$

$$(dp/dL)_{SC} = f_{SC} \rho_C v_{SC}^2 / (2D) \dots\dots\dots (18)$$

For the correlating factor for interfacial friction, Ansari *et al.* found that a correlation developed by Wallis[19] worked well for thin liquid films, while a correlation given by Whalley and Hewitt[20] performed well for thick films. These two correlations are used for the interfacial friction factor for different ranges of entrainment. Thus,

$$Z = 1 + 300\underline{\delta} \qquad for \qquad FE > 0.9 \dots\dots\dots (19)$$

$$Z = 1 + 24\left(\rho_L/\rho_G\right)^{1/3} \qquad for \qquad FE < 0.9 \dots\dots\dots 20)$$

In the superficial friction gradients, superficial core velocity, core density, and core viscosity are defined as follows:

$$v_{SC} = FE v_{SL} + v_{SG} \dots\dots\dots (21)$$

$$\rho_C = \rho_L \lambda_{LC} + \rho_G \left(1 - \lambda_{LC}\right) \dots\dots\dots (22)$$

$$\mu_C = \mu_L \lambda_{LC} + \mu_G \left(1 - \lambda_{LC}\right) \dots\dots\dots (23)$$

λ_{LC} is the no-slip liquid holdup caused by the entrained liquid in the homogeneous mixture of gas and liquid in the core with respect to the core cross section, and is given by

$$\lambda_{LC} = 1 - FE v_{SL} / \left[v_{SG} + FE v_{SL}\right] \dots\dots\dots (24)$$

The entrainment fraction FE given in Eq. 25 was developed by Wallis and was found to be more consistent than other correlations available.

$$FE = 1 - \exp\left[-0.125\left(10000 \frac{v_{SG}\mu_G}{\sigma} \sqrt{\frac{\rho_G}{\rho_L}} \right) - 1.5\right] \dots\dots\dots (25)$$

The friction factors f_F, f_{SL}, and f_{SC} can be obtained from a Moody diagram for the corresponding Reynolds numbers given below:

$$N_{Re,F} = \rho_L v_{SL}\left(1 - FE\right)D / \mu_L \dots\dots\dots (26)$$

$$N_{Re,SL} = \rho_L v_{SL} D / \mu_L \dots\dots\dots (27)$$

$$N_{Re,SC} = \rho_C v_{SC} D / \mu_C \dots\dots\dots (28)$$

At high liquid flow rates, however, the mechanism of bridging occurs, because of the inability of the annular flow configuration to accommodate large amounts of liquid. The criterion given in Eq. 29, which is based on the minimum liquid holdup to form a liquid slug, was proposed[3] for the transition, and considers rhombohedral packing of entrained bubbles (line F in Fig. 1):

$$\left(H_{LF} + \lambda_{LC} A_C / A\right) > 0.12 \dots\dots\dots (29)$$

Flow Behavior Prediction Models

Bubbly Flow Model. The drift flux approach is used to simulate bubbly flow, considering the slippage occurring between the phases and nonhomogenous distribution of the bubbles. Assuming a turbulent velocity profile for the mixture with rising bubbles concentrated more at the center than along the pipe wall, the slip velocity can be expressed as

$$v_s = v_{SG} / \left(1 - H_L\right) - 1.2 v_M \dots\dots\dots (30)$$

If bubble swarm and inclination angle effects are considered rigorously, the following slip velocity expression can be obtained (Appendix A):

$$v_s = 1.53 \left[\frac{g(\rho_L - \rho_G)\sigma}{\rho_L^2} \right]^{0.25} \sqrt{H_L \sin\theta} \quad \text{................ (31)}$$

Combining Eqs. 30 and 31, the following implicit equation for liquid holdup can be found:

$$1.53 \left[\frac{g(\rho_L - \rho_G)\sigma}{\rho_L^2} \right]^{0.25} \sqrt{H_L \sin\theta} = \frac{v_{SG}}{(1-H_L)} - 1.2 v_M \quad \text{..(32)}$$

After determining the holdup by applying a numerical method to Eq. 32, the two-phase mixture properties are calculated from

$$\rho_M = \rho_L H_L + \rho_G(1-H_L) \quad \text{............................ (33)}$$

$$\mu_M = \mu_L H_L + \mu_G(1-H_L) \quad \text{............................ (34)}$$

After calculation of all two-phase parameters for bubbly flow, the total pressure gradient is calculated from the general relation

$$\left(\frac{dp}{dL}\right)_t = \left(\frac{dp}{dL}\right)_e + \left(\frac{dp}{dL}\right)_f + \left(\frac{dp}{dL}\right)_a \quad \text{.................... (35)}$$

The elevation pressure gradient is given by

$$\left(\frac{dp}{dL}\right)_e = \rho_M g \sin\theta \quad \text{................................. (36)}$$

Where ρ_M is obtained from Eq. 33.

The frictional component is given by

$$\left(\frac{dp}{dL}\right)_f = \frac{f_M \rho_M v_M^2}{2D} \quad \text{............................... (37)}$$

Where f_M is the Moody friction factor, determined at a Reynolds number defined as,

$$N_{\text{Re},M} = \rho_M v_M D / \mu_M \quad \text{............................... (38)}$$

The acceleration pressure gradient is neglected for bubbly flow.

Dispersed bubble Flow Model. Since there is a uniform distribution of gas bubbles in the liquid, dispersed bubble flow can be treated as a homogeneous flow. Because of the absence of any slippage between the phases, the pressure drop is estimated by treating the two phases as a pseudo-single phase. By using this simplification,

$$H_L = \lambda_L = v_{SL} / (v_{SL} + v_{SG}) \quad \text{............................ (39)}$$

The two-phase parameters and the pressure drop are calculated by using Eqs. 33-38.

Slug Flow Model. One of the most complex flow patterns with unsteady characteristics is slug flow. Nicklin *et al.*[21] suggested an approach to reduce the slug flow characteristic of

intermittency to periodicity and called this the unit cell approach, which was first clearly formulated by Wallis[19]. Several investigators (Fernandes[22], Sylvester[23], Orell and Rembrandt[24], and Chokshi[5]) also favored this approach.

The Chokshi[5] slug flow model is adopted and significantly modified in this study. A schematic of a typical unit cell under slug flow is shown in Fig. 3.

An overall liquid mass balance over a slug unit moving with a velocity of v_{TB} can be expressed as:

$$\begin{aligned} v_{SL} = &\, v_{TB}(L_{LS}/L_{SU})(1-H_{GLS}) \\ &+ v_{TB}(1-L_{LS}/L_{SU})(1-H_{GTB}) \quad \text{.................... (40)} \\ &- (v_{TB}-v_{LLS})(1-H_{GLS}) \end{aligned}$$

Applying a mixture volumetric balance over the cross section in the liquid slug and assuming constant phase densities, the following expression can be obtain:

$$v_M = v_{LLS}(1-H_{GLS}) + v_{GLS}H_{GLS} \quad \text{.................... (41)}$$

The amount of liquid that moves upstream relative to the bubble nose is the same as the liquid that is overrun by the liquid slug. This exchange can be expressed in volumetric terms as:

$$(v_{TB}-v_{LLS})(1-H_{GLS}) = (v_{TB}-v_{LTB})(1-H_{GTB}) \quad \text{..... (42)}$$

The mass and volume balances given by Eqs. 40-42 contain seven unknowns: H_{GLS}, H_{GTB}, v_{TB}, v_{LTB}, v_{GLS}, v_{LLS} and L_{LS}/L_{SU}. In order to close the mathematical model, four more relations are required; they are provided by four closure relationships for v_{TB}, v_{LTB}, v_{GLS}, and H_{GLS}.

The translational velocity, v_{TB} is generally considered as the sum of the velocity of a single elongated bubble in a stagnant liquid (drift velocity) v_0 and the centerline velocity in the liquid slug.

$$v_{TB} = C_o v_M + v_o \quad \text{................................. (43)}$$

For inclined pipe flow, Bendiksen[15] has proposed the following drift velocity correlation.

$$v_o = (0.35\sin\theta + 0.54\cos\theta)\sqrt{g(\rho_L - \rho_G)D/\rho_L} \quad \text{..... (44)}$$

In this study, the inclination angle dependent C_0 values given by Alves[25] (see Table 1) are used.

The velocity of the liquid film can be correlated with the constant film thickness using an expression developed by Brotz[26] for falling films:

$$v_{LTB} = -9.916\sqrt{gD(1-\sqrt{H_{LTB}})} \quad \text{....................... (45)}$$

The following equation is used to estimate the gas velocity in the liquid slug.

$$v_{GLS} = C_o v_M + C_s \left[\frac{g(\rho_L - \rho_G)\sigma}{\rho_L^2} \right]^{0.25} \sqrt{\sin\theta} \quad \text{....... (46)}$$

Experimentally and theoretically, Zuber et al.[27] proved that for a uniform velocity and void fraction profile, C_0 is very close to unity. Chokshi determined a C_0 value of 1.08, so this value is also used in this study. The recommendation of Zuber et al. of 1.41 for C_s was favored by Chokshi and Tengesdal[7] for their slug flow models, and is also used in this study.

The final and the most important relationship, because of its significant contribution to pressure drop, is the void fraction in the liquid slug, H_{GLS}. Recently, based on an overall gas mass balance in a unit slug, Tengesdal has proposed an improved H_{GLS} closure relationship. This closure relationship has been modified for deviated wells and given as

$$H_{GLS} = \frac{v_{SG}}{1.208v_M + 1.41\left[\dfrac{g(\rho_L - \rho_G)\sigma}{\rho_L^2}\right]^{0.25}\sqrt{\sin\theta}} \quad .... (47)$$

The equation scheme consisting of seven equations, Eqs. 40-43 and 45-47, can be solved for the seven unknowns in the following manner. After solving Eqs. 43 and 47 for v_{TB} and H_{GLS} respectively, Eqs. 41 and 46 are solved for v_{LLS} and v_{GLS}, respectively. Next, Eqs. 42 and 45 are solved explicitly for H_{GTB} and v_{LTB}. Finally, Eq. 40 is solved for the ratio L_{LS}/L_{SU}.

The slug unit is not a homogeneous structure, thereby implying that the axial pressure gradient is not constant. Therefore, the total pressure gradient is given for the entire slug unit. Assuming that the back flowing film gravity balances the shear, pressure remains constant in the bubble region. Therefore, the total pressure gradient over the entire unit is given by:

$$\left(\frac{dp}{dL}\right)_t = \frac{L_{LS}}{L_{SU}}\rho_{LS}\,g\sin\theta + \frac{L_{LS}}{L_{SU}}\frac{f_M\,\rho_{LS}v_M^2}{2D} \quad .... (48)$$

In Eq. 48, the liquid slug density, ρ_{LS}, is given by:

$$\rho_{LS} = \rho_L(1 - H_{GLS}) + \rho_G H_{GLS} \quad .... (49)$$

and f_M is the Moody friction factor determined at a Reynolds number defined by:

$$N_{Re,M} = \rho_{LS}v_M D / \mu_{LS} \quad .... (50)$$

The liquid slug viscosity, μ_{LS}, is given by:

$$\mu_{LS} = \mu_L(1 - H_{GLS}) + \mu_G H_{GLS} \quad .... (51)$$

Although local acceleration and deceleration exist within the slug unit due to local changes in the velocity of the liquid, the acceleration and deceleration effects cancel each other and no net pressure drop occurs due to acceleration over the entire slug unit. Therefore, the acceleration component of the pressure gradient is not considered over a slug unit.

Churn Flow Model. There is no available mechanistic model in the literature to predict hydrodynamic properties of churn flow because of its highly disordered and chaotic nature (Fig. 4). The slug hydrodynamic models are commonly used for

churn flow without any modifications. Tengesdal et al.[4] proposed a modified slug flow hydrodynamic model for churn flow. In this study, the Tengesdal et al. model has been modified for inclined pipes.

The translational velocity, given in Eq. 43, is modified for the flow coefficient. Since churn flow is described as a highly chaotic motion of the gas and liquid under turbulent conditions, the maximum centerline velocity can be approximated by the average mixture velocity. In their drift flux churn flow model, Tengesdal et al. rearranged the Schmidt[28] churn flow data and obtained C_0 as 1.0. Therefore, C_0 is taken as unity. For drift velocity, the Bendikson[15] correlation is used (Eq. 44).

The void fraction in the liquid slug is evaluated with the churn flow data of Schmidt and Majeed[29] and the following expression is obtained:

$$H_{GLS} = \frac{v_{SG}}{1.126v_M + 1.41\left[\dfrac{g\sigma(\rho_L - \rho_G)}{\rho_L^2}\right]^{0.25}\sqrt{\sin\theta}} \quad .... (52)$$

The rest of the churn flow hydrodynamic model is identical to the slug flow model.

Annular Flow Model. Annular flow can be depicted by a liquid film surrounding a gas core with entrained liquid droplets (Fig. 5). Since there is no annular flow model and sufficient experimental data available for inclined pipes, the Ansari et al.[3] vertical annular flow model, which is for uniform film thickness, is adopted in this study.

Since the flow areas are different for the gas core and the film, they can be treated separately. Applying the conservation of momentum independently to the core and the film yields Eqs. 53 and 54, respectively

$$(dp/dL)_C = Z/(1 - 2\underline{\delta})^5(dp/dL)_{SC} + \rho_C g\sin\theta \quad .... (53)$$

$$(dp/dL)_F = (1 - FE)^2\left[64\underline{\delta}^3(1-\underline{\delta})^3\right](f_F/f_{SL})(dp/dL)_{SL}$$
$$- Z/\left[4\underline{\delta}(1-\underline{\delta})(1-2\underline{\delta})^3\right](dp/dL)_{SC} + \rho_L g\sin\theta. \quad (54)$$

Since the pressure drops across the liquid film and the gas core are the same, an implicit equation for $\underline{\delta}$ can be obtained from the simultaneous solution of Eqs. 53 and 54. This gives:

$$Z/\left[4\underline{\delta}(1-\underline{\delta})(1-2\underline{\delta})^5\right](dp/dL)_{SC} - (\rho_L - \rho_C)g\sin\theta$$
$$- (1 - FE)^2\left[64\underline{\delta}^3(1-\underline{\delta})^3\right](f_F/f_{SL})(dp/dL)_{SL} = 0 \quad .... (55)$$

To solve Eq. 55, required correlations and relationships are given in the "Transition From Annular Flow" section. Once $\underline{\delta}$ is found, either Eq. 53 or Eq. 54 can be used to calculate the pressure gradient that includes both the gravitational and frictional components. The acceleration component is neglected, because it is very small compared to the frictional component due to the wavy interface.

Model Evaluation

In order to validate any correlation or mechanistic model, measured data are needed to compare with the predicted results of the correlation or mechanistic model.

In this study, the expanded Tulsa University Fluid Flow Projects (TUFFP) well data bank is used for the performance evaluation. The previously existing well data bank has been expanded by including both the Tulsa University Artificial Lift Projects (TUALP) vertical well data and field data. The expanded TUFFP well data bank consists of 2,052 well cases from various sources covering a wide range of flow parameters.

The performance of the model is also compared with two correlations, and four mechanistic models. In alphabetical order they are: Ansari et al.[3] denoted as ANS in the tables, Aziz et al.[8] denoted as AZIZ, Chokshi[5] denoted as CHO, Hagedorn and Brown[9] denoted as HAG, Hasan and Kabir[6] denoted as HAS and Tengesdal[7] denoted as TENG.

Pressure traverse calculations are usually performed against the flow direction. This is due to the ease of using the available surface data. However, calculations performed in the direction of flow give better results. This is because calculations begin at higher pressures where the flow is often at or close to single phase, and the gradient predictions are more accurate. As pressure decreases, two-phase flow becomes dominant, resulting in relatively less accurate predictions. A well-known shortcoming of the calculations with the flow direction is that the pressure may become negative before reaching the wellhead. This will result in a non-convergent case. Therefore, more non-convergent cases are expected when calculating with the flow direction.

A small number of cases may experience non-convergence even though the system pressures remain positive. This occurs primarily at flow pattern transition boundaries and is due to the different flow characteristics of individual flow patterns. This problem can be overcome by increasing the number of calculation segments and/or by forcing the flow to be in either flow pattern.

Comparison Criteria. A variety of statistical parameters could be used to evaluate the model predictions using the entire data bank. Following are the definitions of the statistical parameters used in this study.

Average Percentage Error

$$E1 = \frac{100}{N} \sum_{i=1}^{N} e_{ri} \quad .... (56)$$

Where the relative error, e_{ri}, is given by

$$e_{ri} = \left(\Delta p_{i,calc} - \Delta p_{i,meas} \right) / \Delta p_{i,meas} \quad .... (57)$$

and N is the number of well cases that successfully converged. E1 indicates the overall trend of the performance relative to the measured pressure drop.

Absolute Average Percentage Error

$$E2 = \frac{100}{N} \sum_{i=1}^{N} |e_{ri}| \quad .... (58)$$

The absolute average percentage error will eliminate the canceling effect of E1. This parameter indicates the general percentage error of the calculations.

Standard Deviation

$$E3 = \sum_{i=1}^{N} \sqrt{(e_{ri} - E1)^2 /(N-1)} \quad .... (59)$$

The standard deviation indicates the scatter of the relative error about the average error.

The statistical parameters described above are based on the errors relative to the measured pressure drop, rather than the actual pressure drop error. Small relative pressure drop errors in a well that experiences a small pressure drop may give a large percentage error even though the pressure drop error is not that far from the actual measurement. To make the statistics independent of the magnitude of the relative pressure drop, a set of statistical parameters based on the error function is used, defined as:

$$e_i = \Delta p_{i,calc} - \Delta p_{i,meas} \quad .... (60)$$

If we replace e_{ri} with e_i in Eqs. 56, 58 and 59, the new parameters can be defined as:

$$E4 = \frac{1}{N} \sum_{i=1}^{N} e_i \quad .... (61)$$

$$E5 = \frac{1}{N} \sum_{i=1}^{N} |e_i| \quad .... (62)$$

$$E6 = \sum_{i=1}^{N} \sqrt{(e_i - E4)^2 /(N-1)} \quad .... (63)$$

Ansari et al.[3] recommended the use of a composite error factor, denoted as RPF (Relative Performance Factor) for comparison among a group of methods. The minimum and maximum possible values for RPF are 0 and 6, corresponding to the best and the worst prediction performance, respectively. RPF is expressed as

$$RPF = \frac{|E1| - |E1_{mn}|}{|E1_{mx}| - |E1_{mn}|} + \frac{E2 - E2_{mn}}{E2_{mx} - E2_{mn}} + \frac{E3 - E3_{mn}}{E3_{mx} - E3_{mn}}$$
$$+ \frac{|E4| - |E4_{mn}|}{|E4_{mx}| - |E4_{mn}|} + \frac{E5 - E5_{mn}}{E5_{mx} - E5_{mn}} + \frac{E6 - E6_{mn}}{E6_{mx} - E6_{mn}} \quad (64)$$

Overall Evaluation. The overall evaluation of the current mechanistic model was accomplished using the expanded TUFFP well data bank. The current model performed best compared to all other models and correlations regardless of the

calculation direction. The statistical results are presented in Tables 2-9. The first line of each table identifies the methods. The statistical errors E1-E6 are given in lines 2-7, respectively. The eighth line gives the relative performance factor. The ninth line reports the number of non-convergence cases.

Table 2 reports the errors for predicting pressure drop for all 2,052 well cases in the TUFFP data bank. Based on RPF values, the current model gives the best result. The model has all the lowest error values, except for E1 and E4. The lowest results for these parameters are given by Hasan and Kabir[9] and Tengesdal[7], respectively. The small values of E1 and E4 can be attributed to the canceling effect of large positive and negative errors. The model exhibits a slightly under-predictive trend.

The performance of the current model for 623 deviated well cases is shown in Table 3. The model gives the best result, except for E3 and E6. The Chokshi[5] model has better values for these parameters. Both of these parameters are the standard deviation in percentage and psi, respectively, and do not indicate how close the predictions are to actual data but rather represents the consistency.

The performance of the current model for 1,429 vertical well cases is shown in Table 4. The model gives the best result, followed by the Tengesdal mechanistic model. The model has all the lowest error values, except for E1 and E4. The Hagedorn and Brown[9] correlation has the lowest values for these parameters.

An over-predicting trend of a model or correlation for one flow pattern may often be offset by an under-predicting trend for other flow patterns, resulting in an overall good performance of the model or correlation. Therefore, individual flow pattern models should be evaluated separately. For such an evaluation, the flow pattern prediction model, proposed in this study, is used to cull the well cases into subgroups for each flow pattern.

The performance of the current model for 1,267 well cases containing 100% slug flow is shown in Table 5. The model gives the best result, except for the E1 and E4 parameters.

A conclusive evaluation of the proposed model requires a certain number of well cases for a particular flow pattern. There were only 36 wells that had churn flow over the entire wellbore. Therefore, an attempt was made to evaluate the model by considering well cases that have churn flow over at least 75% of the well length. This resulted in 46 well cases. The performance of the proposed churn hydrodynamic model is shown in Table 6. The proposed model and the Tengesdal model give almost identical and the best results. The model differs from the Tengesdal model by modification for inclined pipes and use of a different flow coefficient for Taylor Bubble velocity. Since there are no inclined wells in these 46 well cases, both models exhibit almost the same performance with slightly better results for the current model. From Table 6, one can clearly see that both models outperform all the other models by a considerable margin, thus giving a much lower relative performance factor.

There are only eight 100% bubble flow cases. Therefore, well cases that have bubble flow over at least 75% of their length have been considered. This has resulted in the 44 well cases for the evaluation of the bubble flow model. The performance of the proposed bubble flow model is shown in Table 7. Except for E1 and E4, the proposed model gives the lowest statistical error values and the lowest RPF value.

The performance of the model for 71 well cases containing 100% annular flow is shown in Table 8. The model and the Tengesdal and Ansari et al.[3] mechanistic models yield the same best results, with a relative performance factor of 0.0.

The performance of the model for all 2,052 well cases is shown in Table 9 for the calculations performed against the flow direction. The model has the lowest error values for E2, E5 and RPF. The lowest results for the other parameters are given by Chokshi (E1), Hagedorn and Brown (E3), Tengesdal (E6) and Hasan and Kabir[6] (E4).

Conclusions

A modeling study of two-phase flow in inclined pipes has been conducted. A new comprehensive mechanistic model for vertical and inclined upward flow is proposed for flow pattern and flow characteristic predictions. The model considers five flow patterns: bubbly, dispersed bubble, slug, churn and annular flows.

Ansari et al.[3] for annular flow, Taitel et al.[2] for dispersed bubble, Tengesdal et al.[4] model for churn flow and a new transition model for bubbly flow constitute the flow pattern prediction models.

The mechanistic model consists of a homogeneous hydrodynamic model for dispersed bubble flow, a new model for bubbly flow, a modified Chokshi[5] model for slug flow, the Ansari et al. model for annular flow, and a modified Tengesdal et al. model for churn flow.

Comparisons of pressure drop predictions with the TUFFP expanded well data bank containing 2,052 well cases from field and laboratory experiments have been made. Compared with two correlations and four mechanistic models, the model gives the best results regardless of calculation direction.

On the basis of the overall performance of the model, it should be used in preference to other models for two-phase flow calculations in wells.

Nomenclature

C_0 = flow coefficient
C_s = flow coefficient
D = pipe diameter
d = bubble diameter
e_i = error function given by Eq. 60
er_i = relative error function given by Eq. 57
$E1$ = average percentage error
$E2$ = absolute average percentage error
$E3$ = standard deviation in percentage
$E4$ = average error
$E5$ = absolute average error
$E6$ = standard deviation
f = friction factor

FE = entrainment fraction
g = gravity acceleration
H = holdup fraction
L = length
N = number
p = pressure
v = velocity
Y, X = Lockhart and Martinelli parameter
Z = correlating factor for interfacial friction

Greek letters

α = void fraction
δ = ratio of film thickness to diameter
μ = dynamic viscosity
θ = angle from horizontal
ρ = density
λ = no-slip holdup
σ = surface tension

Subscripts

a = acceleration
bs = bubble rise velocity
D = drift
C = core
$calc$ = calculated value
CB = critical bubble diameter for migration
CD = critical bubble diameter for deformation
e = elevation
f = friction
F = film
G = gas
GLS = gas in liquid slug
GTB = gas in Taylor bubble
L = liquid
LF = liquid film
LLS = liquid in liquid slug
LS = liquid slug
LTB = liquid in Taylor bubble
$meas$ = measured value
mn = minimum
mx = maximum
M = mixture, medium, Moody
Re = Reynolds number
S = slip
SL = superficial liquid
SC = superficial core
SG = superficial gas
SU = slug unit
t = total
TB = Taylor bubble in flowing liquid
0 = rise velocity of Taylor bubble

Acknowledgments

References

1. Barnea, D.: "A Unified Model for Predicting Flow-Pattern Transition for the Whole Range of Pipe Inclinations," *Int. J. Multiphase Flow* (1987), **13,** 1-12.
2. Taitel, Y., Barnea, D., and Dukler, A. E.: "Modeling Flow Pattern Transitions for Steady State Upward Gas-Liquid Flow in Vertical Tubes," *AIChE J.* (1980), **26**, 345-354.
3. Ansari, A. M., Sylvester, N. D, Sarica, C, Shoham, O. and Brill, J. P.: "A Comprehensive Mechanistic Model for Upward Flow in Pipes," *SPEPF J* (May 1994), 217-226.
4. Tengesdal, J. O., Kaya A. S. and Sarica C.: "An Investigation of Churn Flow: Flow Pattern Transition and Hydrodynamic Modeling Considerations," Submitted to *SPE J.* (1998).
5. Chokshi, R. N.*: "Prediction of Pressure Drop and Liquid Holdup in Vertical Two-Phase Flow Through Large Diameter Tubing,"* Ph.D. Dissertation, The University of Tulsa, (1994).
6. Hasan, A. R. and Kabir, C. S.: "Predicting Multiphase Flow Behavior in a Deviated Well," *SPEPE J.* (Nov. 1988), 474-482
7. Tengesdal, J. Ø.: *"Predictions of Flow Patterns, Pressure Drop, and Liquid Holdup in Vertical Upward Two-Phase Flow,"* MS Thesis, The University of Tulsa, (1998).
8. Aziz, K., Govier, G. W., and Fogarasi, M.: "Pressure Drop in Wells Producing Oil and Gas," *JCPT* (July-Sept 1972), 38-47.
9. Hagedorn, A. R. and Brown, K. E.: "Experimental Study of Pressure Gradients Occurring during Continuous Two-Phase flow in Small Diameter Vertical Conduits," *JPT* (April 1965), **17**, 475-484.
10. Shoham, O.: "*Flow Pattern Transitions and Characterization in Gas-Liquid Two-Phase Flow in inclined Pipes,*" Ph.D. Dissertation, Tel-Aviv University, Ramat-Aviv, Israel, (1982).
11. Barnea, D., Shoham, O., Taitel, Y. and Dukler, A. E.: "Gas-Liquid Flow in Inclined Tubes: Flow Pattern Transitions for Upward Flow," *Chem. Eng. Sci.* (1985), **40**, 131-136.
12. Harmathy, T. Z.: "Velocity of Large Drops and Bubbles in Media of Infinite or Restricted Extent," *AIChe J.* (1960) **6**, 281.
13. Hinze, J. O.: "Fundamentals of the Hydrodynamic Mechanism of Splitting in Dispersion Processes," *AIChE J.* (1955) **1**, 289-295.
14. Barnea, D.: "Transition From Annular and From Dispersed Bubble Flow- Unified Models For Whole Range Of Pipe Inclinations," *Int. J. Multiphase Flow* (1986), **12**, 733-744.
15. Bendiksen, K. H.: "An Experimental Investigation of The Motion of Long Bubbles In Inclined Tubes, " *Int. J. Multiphase Flow* (1984) **10**, 467-483.
16. Owen, D. G.: "*An Experimental and Theoretical Analysis of Equilibrium Annular Flow,*" Ph.D. Thesis, Univ. of Birmingham, U.K.
17. Kaya, A. S., Chen, X. T., Sarica, C. and Brill, J. P.: "Investigation of Transition from Annular to Intermittent Flow in Pipes," *J. Energy Res. Tech.* (May 1999).
18. Lockhart, R. W. and Martinelli, R. C.: "Proposed Correlation of Data for Isothermal Two-Phase Two-Component Flow in Pipes," *Chem. Eng. Prog.* (Jan. 1949) **45**, No.1, 39-48.
19. Wallis, G. B.: *One-Dimensional Two-Phase Flow*, McGraw-Hill (1969).
20. Whalley, P. B. and Hewitt, G. F.: "The Correlation of Liquid Entrainment Fraction and Entrainment Rate in Annular Two-Phase Flow," UKAEA Report, AERE-R9187, Harwell, (1978).
21. Nicklin, D. J., Wilkes, J. O. and Davidson, J.F.: "Two Phase Flow in Vertical Tubes," *Trans. Inst. Chem. Engrs.* (1962), **40**, 61-68.

22. Fernandes, R. C.: "*Experimental and Theoretical Studies of Isothermal Upward Gas-Liquid Flows in Vertical Tubes, Ph.D. Dissertation,*" The University of Houston, (1981).

23. Sylvester, N. D.: "A Mechanistic Model for Two-Phase Vertical Slug Flow in Pipes," *J. Energy Res. Tech.* (1987), **109**, 206.

24. Orell, A., and Rembrandt, R.: "A Model for Gas-Liquid Flow in Vertical Tubes," *Ind. Eng. Chem. Fundam.* (1986), **25**, 196-206.

25. Alves, I. N.: "*Slug Flow Phenomena in Inclined Pipes, Ph.D. Dissertation,*" The University of Tulsa, Tulsa, Oklahoma, 1991.

26. Brotz, W.: "Uber die Vorausberechnung der Absorptionsgesch-windigkeit von Gasen in Stromenden Flussigkeitsschichten," *Chem. Ing. Tech.* (1954), **26**, 470.

27. Zuber, N., Staub, G., Bijward, G. and Kroeger, P. G.: "Steady State and Transient Void Fraction in Two-Phase Flow Systems," 1, Report EURAEC-GEAP-5417, General Electric Co., San Jose, CA, Jan. (1967).

28. Schmidt, Z.: "*Experimental Study of Two-Phase Flow in a Pipeline-Riser Pipe System,*" Ph.D. Dissertation, The University of Tulsa, (1977).

29. Majeed, G. H.: "*A Comprehensive Mechanistic Model for Vertical and Inclined Two-Phase Flow,*" Dr. Sci., The University of Baghdad, Iraq, (1997).

30. Peebles, F. N. and Garber, H. J.: "Studies on the Motion of Gas Bubbles in Liquid," *Chem. Eng. Prog.* (1953), **49**, 88.

Appendix A - Relative Motion of Bubble in a Liquid Column

The relative velocity of a bubble located in a swarm of bubbles can be evaluated by considering the drag and buoyancy forces acting on a single bubble under the assumption that bubbles do not interfere with each other.

For a single bubble, the drag force can be expressed as

$$F_D = C_D \left(\pi d^2 / 4 \right) \rho_L v_{bs}^2 / 2 \quad \text{.......................... (A-1)}$$

The buoyancy force is given by

$$F_B = (\rho_M - \rho_G) \sin\theta \iint (z_1 - z_2) dx dy \quad \text{................. (A-2)}$$

Where z_2 and z_1 are the coordinates on the surface of the bubble, and ρ_M is the medium density in which a solitary gas bubble rises. The medium density can be expressed in a rigorous way as follows:

$$\rho_M = \frac{1}{A} \left[\rho_L \int_0^r 2\pi r H_L(r) dr + \rho_G \int_0^r 2\pi r [1 - H_L(r)] dr \right] \quad \text{.... (A-3)}$$

Assuming uniform bubble distribution across the pipe cross section, mixture density can be written as

$$\rho_M = (\rho_L - \rho_G) H_L + \rho_G \quad \text{.......................... (A-4)}$$

When Eq. A-4 is substituted into Eq. A-2 and bubbles are assumed to be spherical, the buoyancy force can be evaluated as

$$F_B = (\rho_L - \rho_G) H_L g \frac{\pi d^3}{6} \sin\theta \quad \text{...................... (A-5)}$$

The equilibrium between buoyancy and drag forces gives

$$v_{bs} = \sqrt{\frac{4}{3} \frac{(\rho_L - \rho_G)g}{\rho_L C_D} d H_L \sin\theta} \quad \text{..................... (A-6)}$$

Where C_D is the drag coefficient, which depends on the shape of the bubble. Peebles and Garber[30], and Harmathy[12] proposed different drag coefficients:

$$C_D = \begin{cases} 0.95\sqrt{\dfrac{g(\rho_L - \rho_G)d^2}{\sigma}} & Peebles\ \&\ Garber \\ 0.575\sqrt{\dfrac{g(\rho_L - \rho_G)d^2}{\sigma}} & Harmathy \end{cases} \quad \text{... (A-7)}$$

Substituting Eqs. A-7 into A-6, one can obtain:

$$v_s = 1.53 \left[\frac{g(\rho_L - \rho_G)\sigma}{\rho_L^2} \right]^{0.25} \sqrt{H_L \sin\theta} \quad \text{............... (A-8)}$$

Where, $C_s = 1.18$ for Peebles and Garber and 1.53 for Harmathy. In this study, Harmathy's $C_s = 1.53$ is used, since Peebles and Garber obtained their $C_s = 1.18$ empirical coefficient from experimental tests for relatively large spherical cap shaped bubbles.

Table 1: Flow Coefficients for Different Inclination Angle Ranges

Angle	C_0
10°-50°	1.05
50°-60°	1.15
60°-90°	1.25

Table 2: Evaluation Based on Entire Databank (2,052 Cases)

Corr/ Model	MOD	HAG	CHO	TENG	AZIZ	HAS	ANS
E_1 (%)	-1.3	-0.8	-2.3	-1.2	-2.4	**-0.1**	-5.1
E_2 (%)	**9.1**	9.9	9.9	9.2	12.9	13.3	12.5
E_3 (%)	**12.7**	14.1	13.9	12.9	17.8	19.1	16.9
E_4 (Psi)	-3.4	-23.9	-6.3	**-1.2**	-16.2	-22.2	1.4
E_5 (Psi)	**73.6**	88	76.1	74.7	100.2	109.8	86.9
E_6 (Psi)	**128.7**	149.1	131	129.4	161.9	178.8	139.2
RPF (-)	**0.216**	1.737	0.886	0.257	3.597	4.264	2.673
N.C (-)	54	74	50	69	32	207	**21**

Table 3: Evaluation of Deviated Well Data (623 Cases)

Corr/ Model	MOD	HAG	CHO	TENG	AZIZ	HAS	ANS
E_1 (%)	**1**	-2.5	1.6	2	-2	-1.5	2.9
E_2 (%)	**6.2**	6.4	6.3	6.5	9	8.8	7.5
E_3 (%)	8.8	9.2	**8.7**	8.8	11.4	12.1	9.5
E_4 (Psi)	**7.4**	-61.2	14.2	18.7	-20.8	-17.7	49.3
E_5 (Psi)	**106.4**	111.2	107	110.3	144	142.9	128.4
E_6 (Psi)	163.6	167.6	**162.8**	164.1	191.2	198.9	171.8
RPF (-)	**0.037**	1.793	0.303	0.675	3.745	3.867	2.588
N.C (-)	32	25	34	46	**4**	27	15

Table 4: Evaluation of Vertical Well Data (1,429 Cases)

Corr/ Model	MOD	HAG	CHO	TENG	AZIZ	HAS	ANS
E_1 (%)	-2.3	**-0.1**	-3.9	-2.5	-2.5	0.5	-8.5
E_2 (%)	**10.3**	11.4	11.4	10.4	14.6	15.5	14.7
E_3 (%)	**13.9**	15.7	15.3	14	20	21.6	18.2
E_4 (Psi)	-7.9	**-7.7**	-14.9	-9.4	-14.2	-24.4	-19.1
E_5 (Psi)	**59.8**	78	63.2	60.1	80.8	93.9	69.2
E_6 (Psi)	110.5	137.2	114.2	111.2	147.2	168.5	117
RPF (-)	**0.267**	1.376	1.149	0.37	3.24	4.323	3.006
N.C (-)	22	49	16	23	28	180	**6**

Table 5: Evaluation of Slug Flow Model (Flow over 100% length of pipe) (1,267 Cases)

Corr/ Model	MOD	HAG	CHO	TENG	AZIZ	HAS	ANS
E_1 (%)	-1.7	**-0.9**	-1.8	-1.7	-0.8	3.8	-5.7
E_2 (%)	**10.4**	10.8	10.7	10.6	13.8	14.5	14.3
E_3 (%)	**13.9**	15.2	14.3	14.1	18.6	19.8	17.6
E_4 (Psi)	-2.3	-19.8	-2.7	**-0.1**	-0.2	**0.1**	9.5
E_5 (Psi)	**70.4**	80.8	71.8	71.4	91.5	99.4	87.8
E_6 (Psi)	**122.6**	146	124	122.9	146.6	161.1	134.3
RPF (-)	**0.172**	1.582	0.415	0.231	2.841	4.231	3.255
N.C (-)	4	17	5	7	15	162	**2**

Table 6: Evaluation of Churn Flow Model (Flow over 75% length of pipe) (46 Cases)

Corr/ Model	MOD	HAG	CHO	TENG	AZIZ	HAS	ANS
E_1 (%)	-3.1	-4.8	-26.7	**0.8**	-27.8	-35.4	-32.2
E_2 (%)	**12.7**	15.6	27.2	**12.7**	37.2	36.3	36.6
E_3 (%)	**15.4**	18.6	13.1	16.5	30.2	21.6	22.3
E_4 (Psi)	-5.9	9.8	-41.4	**-0.6**	-19	-39	-30.1
E_5 (Psi)	**20**	25.6	42.4	20.8	53.5	40.6	47.5
E_6 (Psi)	**35.7**	55.1	51	37	71.9	47.3	55.5
RPF (-)	0.34	1.218	3.213	**0.251**	4.714	4.169	4.229
N.C (-)	**0**	**0**	**0**	**0**	**0**	3	**0**

Table 7: Evaluation of Bubble Flow Model (Flow over 75% length of pipe) (44 Cases)

Corr/ Model	MOD	HAG	CHO	TENG	AZIZ	HAS	ANS
E_1 (%)	-0.7	-1.6	**-0.4**	-0.8	-3.9	-3.8	-0.6
E_2 (%)	**3**	4.1	3.4	3.2	5.3	5.3	3.3
E_3 (%)	**3.9**	4.7	4.4	4.1	6.3	7.2	4
E_4 (Psi)	-10	-18.8	**-0.1**	-9.4	-88.9	-95.6	-10
E_5 (Psi)	**61.5**	74.1	70.2	63.4	116.5	125.3	70.4
E_6 (Psi)	**83.9**	98.3	97.5	88.2	167.3	186.4	93.4
RPF (-)	**0.188**	1.584	0.595	0.405	5.294	5.958	0.57
N.C (-)	1	3	1	1	**0**	**0**	**0**

Table 8: Evaluation of Annular Flow Model (Flow over 100% length of pipe) (71 Cases)

Corr/ Model	MOD	HAG	CHO	TENG	AZIZ	HAS	ANS
E_1 (%)	**-0.9**	10.6	-4.5	**-0.9**	4.3	-18.7	**-0.9**
E_2 (%)	**9.5**	15.8	10.7	**9.5**	12.1	19.4	**9.5**
E_3 (%)	**12.4**	16.4	15.1	**12.4**	16.1	13.2	**12.4**
E_4 (Psi)	**-14.6**	73.3	-46.8	**-14.6**	26.5	173.9	**-14.6**
E_5 (Psi)	**87**	130	98.2	**87**	99.2	177.1	**87**
E_6 (Psi)	**131.1**	145.8	153.5	**131.1**	135.7	166.2	**131.1**
RPF (-)	**0**	1.963	1.249	**0**	1.019	2.897	**0**
N.C (-)	1	1	1	1	1	**0**	1

Table 9: Evaluation Based on Entire Data bank (Against Flow Direction) (2,052 Cases)

Corr/ Model	MOD	HAG	CHO	TENG	AZIZ	HAS	ANS
E_1 (%)	0.9	-1.5	**-0.1**	1.2	-2	5.2	-5.2
E_2 (%)	**15.1**	**15.1**	16.3	15.2	23.5	23.3	20
E_3 (%)	21.9	**20.6**	23.6	21.8	32	33.5	26
E_4 (Psi)	10.7	-50.6	8.9	15.2	-24.8	**-3.7**	15.1
E_5 (Psi)	**126.5**	148.9	129.6	127.4	188.4	185.8	151
E_6 (Psi)	215.7	253.2	217.1	**214.3**	293.7	296.6	239.1
RPF (-)	**0.257**	1.449	0.514	0.334	4.223	4.338	2.223
N.C (-)	8	**0**	1	9	**0**	**0**	16

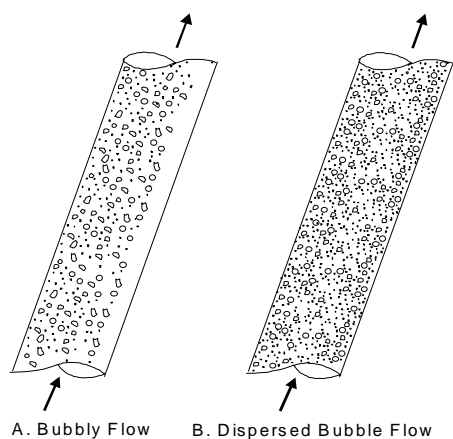Fig. 1: Flow Pattern Map (90°, 5.08 cm pipe)

Fig. 2: Bubble Flow Configuration in Upward Inclined Two-Phase Flow
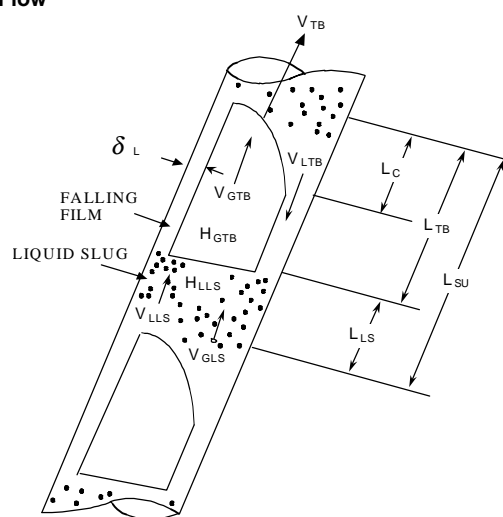

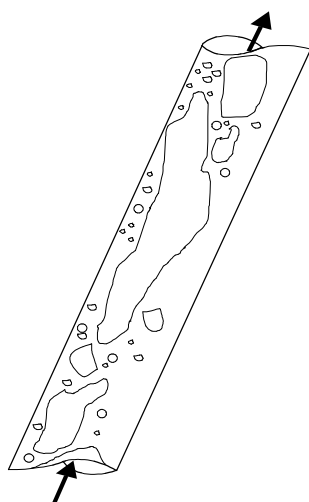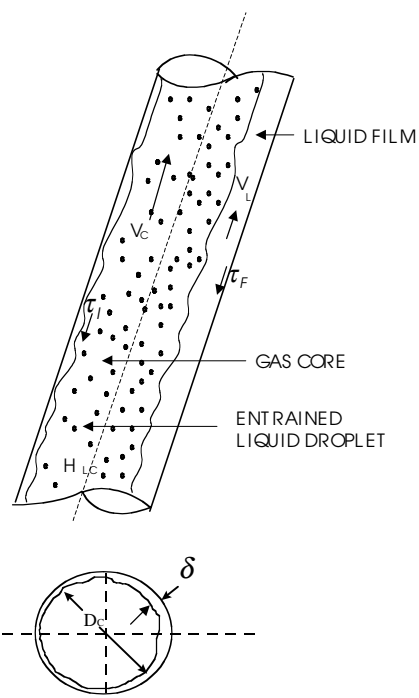**Fig. 3: Slug Flow Configuration in Upward Inclined Two-Phase Flow**

Fig. 5: Annular Flow Configuration in Upward Inclined Two-Phase Flow

Fig. 4: Churn Flow Configuration in Upward Inclined Two-Phase Flow